CrossMark

ORIGINAL ARTICLE

Afferent and efferent connections of C1 cells with spinal cord or hypothalamic projections in mice

Ruth L. Stornetta[1] · M. Andrews Inglis[1] · Kenneth E. Viar[1] · Patrice G. Guyenet[1]

Abstract The axonal projections and synaptic input of the C1 adrenergic neurons of the rostral ventrolateral medulla (VLM) were examined using transgenic dopamine-beta hydroxylase Cre mice and modified rabies virus. Cre-dependent viral vectors expressing TVA (receptor for envelopeA) and rabies glycoprotein were injected into the left VLM. EnvelopeA-pseudotyped rabies-EGFP glycoprotein-deficient virus (rabies-EGFP) was injected 4–6 weeks later in either thoracic spinal cord (SC) or hypothalamus. TVA immunoreactivity was detected almost exclusively (95 %) in VLM C1 neurons. In mice with SC injections of rabies-EGFP, starter cells (expressing TVA + EGFP) were found at the rostral end of the VLM; in mice with hypothalamic injections starter C1 cells were located more caudally. C1 neurons innervating SC or hypothalamus had other terminal fields in common (e.g., dorsal vagal complex, locus coeruleus, raphe pallidus and periaqueductal gray matter). Putative inputs to C1 cells with SC or hypothalamic projections originated from the same brain regions, especially the lower brainstem reticular core from spinomedullary border to rostral pons. Putative input neurons to C1 cells were also observed in the nucleus of the solitary tract, caudal VLM, caudal spinal trigeminal nucleus, cerebellum, periaqueductal gray matter and inferior and superior colliculi. In sum, regardless of whether they innervate SC or hypothalamus, VLM C1 neurons receive input from the same general brain regions. One interpretation is that many types of somatic or internal stimuli recruit these neurons en bloc to produce a stereotyped acute stress response with sympathetic, parasympathetic, vigilance and neuroendocrine components.

Introduction

The adrenergic C1 neurons of the rostral ventrolateral medulla (VLM) regulate the cardiovascular system and the hypothalamic-pituitary axis (HPA), but more recent evidence suggests that these cells have a wider role in preparing the body for emergency situations beyond challenges to blood pressure (Guyenet et al. 2013). The C1 neurons can be divided into several subsets based on peptide content, receptors, vesicular transporters, projection patterns and conduction velocity (Farnham et al. 2008; Koji et al. 2008; Lonergan et al. 2003; Guyenet et al. 2004; Stornetta et al. 1990, 2001; Stornetta 2009; Aicher et al. 2001; Schreihofer and Guyenet 1997; Sawchenko and Bohn 1989; Sevigny et al. 2008; Comer et al. 1998). A common classification is based on whether these neurons have a hypothalamic or a spinal projection. In rats, the spinally projecting C1 neurons are located more rostrally, about half of them have lightly myelinated axons and most lack NPY, whereas hypothalamic-projecting C1 neurons reside more caudally within the VLM, have slower conduction velocities and co-express NPY (Stornetta et al. 1999; Verberne et al. 1999; Tucker et al. 1987; Sawchenko et al. 1985).

The bulbospinal C1 neurons directly innervate the sympathetic preganglionic neurons and regulate

✉ Ruth L. Stornetta
   stornetta@virginia.edu; rs3j@virginia.edu

1   Department of Pharmacology, University of Virginia Health System, 1340 Jefferson Park Avenue, P.O. Box 800735, Charlottesville, VA 22908-0735, USA

sympathetic tone, most notably to the cardiovascular system (Ross et al. 1981, 1984; Abbott et al. 2009, 2012; Marina et al. 2011). The C1 neurons with spinal projections may consist of several subsets that differentially control sympathetic tone to various cardiovascular organs or vascular beds (McAllen et al. 1997; Mueller et al. 2011). However, stimulation of the C1 neurons also causes arousal, sighs, stimulates breathing and activates vagal efferents, thus demonstrating that these neurons are involved in more than just cardiovascular control (Abbott et al. 2014a; Holloway et al. 2013; Burke et al. 2014; Guyenet et al. 2013). The C1 neurons projecting to hypothalamus have been implicated in feeding, glucose regulation, stress and immune responses (Li et al. 2015a; Ritter et al. 1998, 2001; Dayas et al. 2001; Ericsson et al. 1994, 1997; Li et al. 1996, 2009, 2015b).

Based on fos expression, many stimuli seem capable of activating all or most C1 neurons, for example hemorrhage, diving and hypoxia (McCulloch and Panneton 2003; Erickson and Millhorn 1994; Panneton et al. 2012; Chan and Sawchenko 1994). These stimuli elicit complex physiological responses involving both sympathetic and parasympathetic efferents (Paton et al. 2005). In short, the various subsets of C1 neurons could have many common inputs, but each set could contribute to a different physiological response by innervating distinct brain regions. This view remains speculative.

The bulbospinal C1 neuron collaterals have been investigated most extensively. Many of these C1 cells also project to the dorsal vagal complex, parabrachial nucleus, locus coeruleus, periaqueductal gray, and hypothalamus (Huangfu et al. 1992; Verberne et al. 1999; Mtui et al. 1995; Lipski et al. 1995; Kwiat and Basbaum 1990; Haselton and Guyenet 1990). The C1 neurons that project to the hypothalamus innervate many nuclei within this region and the basal forebrain (Petrov et al. 1993; Sawchenko and Swanson 1982; Li et al. 2015b) and may also have collaterals elsewhere in the brain; however, these projections have not been identified.

The purpose of the present study was to identify the inputs and the axonal projections of two distinct populations of C1 neurons: those that innervate the spinal cord and those that innervate the hypothalamus. The monosynaptic inputs to these cells were identified using the modified rabies virus method designed by Callaway (Callaway and Luo 2015; Wickersham et al. 2007a, b). To enter into neurons, this modified rabies virus requires a receptor (TVA) that is not expressed in mammals. The modified rabies also lacks the glycoprotein (RG) necessary for retrograde trans-synaptic transport (Wickersham et al. 2007a). To introduce TVA and RG selectively into C1 neurons, we used Cre-dependent adeno-associated vectors in a transgenic mouse that expresses Cre only in catecholaminergic

neurons. We injected the modified rabies virus into either the spinal cord or the hypothalamus. In this fashion, we were able to identify the collaterals and the monosynaptic inputs of each subset of C1 neurons.

Methods

Strategy

In order to restrict rabies expression to C1 neurons based on their projection pattern, first both TVA, the receptor for the envelopeA-pseudotyped rabies virus and the rabies G-protein which is necessary for the rabies virus to bud out and travel across the synapse were introduced in a Cre-dependent manner (using FLEX constructs) specifically into the catecholaminergic neurons of the ventrolateral medulla using a mouse with Cre expression restricted to DβH-containing neurons (Abbott et al. 2013; Holloway et al. 2013; Stornetta et al. 2013). After 4–6 weeks to allow time for the viral expression of TVA to extend to the terminal fields of the transduced neurons, the envelopeA-pseudotyped rabies virus was introduced into the terminal fields of C1 neurons either in the spinal cord or in the hypothalamus. The only possibility for this modified rabies virus to enter and infect the neurons is through binding with the TVA on the axons and terminals of the C1 neurons as the cell bodies and dendrites of these neurons do not extend into the hypothalamus or spinal cord.

Animals

We used a total of 30 (16 female, 14 male) dopamine beta hydroxylase (DβH)–Cre mice (Strain Tg(Dbh-cre)KH212G-sat/MMUCD; Stock 032081-UCD; Mutant Mouse Regional Resource Center, San Diego, CA, USA). Mice were kept as hemizygous on a C57BL/6J background (JAX Stock#000664, Jackson Laboratory; Bar Harbor, ME, USA). All procedures conformed to the NIH Guide for the Care and Use of Laboratory Animals and were approved by the University of Virginia Animal Care and Use Committee. Animals were housed under standard 12 h light/dark cycle with ad libitum access to food and water.

Viral constructs

The following recombinant adeno-associated viral vectors serotype 5 (rAAV-5) were obtained from the University of North Carolina Vector Core (Chapel Hill. NC, USA): CAG-FLEX-RG [titer 3×10^{12} transforming units (tu)/ml] and EF1alpha-FLEX-TVA-mCherry (titer 3×10^{12} tu/ml). EnvA-deltaG-B19-EGFP rabies vector (titer between 3.0×10^7–4.3×10^8 tu/ml) was obtained from the Salk

Institute Gene Transfer, Targeting and Therapeutics Facility (La Jolla, CA, USA).

Surgery and perfusions

Viral vector microinjections were performed under aseptic conditions in mice anesthetized with a mixture of ketamine (100 mg/kg) and dexmedetomidine (0.2 mg/kg; i.p.) as previously described (Abbott et al. 2013). Adequate anesthesia was judged by the absence of the corneal and hindpaw withdrawal reflexes. Additional anesthetic was administered if necessary (20 % of the original dose, i.p.). Anesthetized mice were placed into a modified stereotaxic device (David Kopf, Tujunga, CA, USA) with the bite bar set at −2 mm from horizontal. Body temperature was maintained at 37 °C with a thermostatically controlled heating pad placed under the mouse. Viral vectors were loaded into a glass micropipette with tip 25–30 μm. Two to three 130 nl injections of a mixture of CA-FLEX-RG and EF1alpha-FLEX-TVA-mCherry rAAV5s (mixed in equal volumes) were aligned 0.2 mm apart in the rostrocaudal direction and located on average 1.4 mm lateral to the midline, 1.2 mm caudal to lambda and 5.5 mm ventral to the cerebellar surface. Individual adjustments of up to 300 μm in all directions were made based on the location of the facial motor nucleus which was identified by antidromic field potentials in each mouse (Abbott et al. 2014b). Four to six weeks later, mice were re-anesthetized and re-operated as described above. EGFP rabies vector was injected into the hypothalamus (2–3 × 130 nl; stereotaxic coordinates: 0.5 mm lateral, 0.8, 1.2 and 1.6 mm caudal to bregma and 5 mm below the dura) or the spinal cord (segments T2–T3; 0.3 mm lateral to the midline and 0.5 mm below the dorsal surface). After 5–10 days, animals were anesthetized and perfused transcardially with 10 ml heparinized phosphate buffered saline followed by 70–80 ml of 4 % paraformaldehyde. Brains were removed and placed in fixative for 24–48 h at 4 °C.

Immunohistochemistry

Thirty micron brain sections were made in the transverse plane on a vibrating microtome and stored in a cryoprotectant solution (30 % ethylene glycol, 20 % glycerol, 50 % 100 mM sodium phosphate buffer, pH 7.4) at −20 °C until further processing. Sections were reacted in a one in three series using a standard free-floating immunohistochemical protocol as previously described (Stornetta et al. 2013). TVA-mCherry was identified with a rabbit anti-DsRed antibody (1:500, #632496 Clontech laboratories, Inc., Mountain View, CA, USA). Rabies-EGFP was identified with a chicken anti-GFP antibody (1:1,000; AVES labs, Tigard, OR, USA) followed by Alexa

488-tagged donkey anti-chicken IgY (1:200, Jackson). TH was identified with a sheep antibody (1:2000, Millipore) followed by a Dylight 649-tagged donkey anti-sheep IgG (1:200, Jackson).

Antibody characterization

Chicken anti-GFP antibody (Aves #GFP-1020) was raised against recombinant GFP and extracted from egg yolk IgY fractions. Antibodies were analyzed by Western blot analysis (1:5000 dilution) and immunohistochemistry (1:500 dilution) using transgenic mice expressing the GFP gene product (manufacturer's information). No labeling was seen in brains from mice without rabies virus injections.

Sheep anti-TH polyclonal antibody (Millipore #AB1542) was raised against native TH from rat pheochromocytoma. Western blot analysis using a 1:1000 dilution of antibody on 10 μg of mouse brain tissue lysates revealed a single band at the predicted molecular weight of ∼60 kDa. Positive controls included caudate striatum and adrenal gland. No staining was observed in liver (manufacturer's information). The pattern of labeling matched the known location of brainstem catecholaminergic neurons (Chen et al. 2010; VanderHorst and Ulfhake 2006).

Rabbit anti-DsRed antibody (Clontech #632496) was raised against DsRed-express, a variant of *Discosoma* sp. red fluorescent protein that recognizes both N- and C-terminal fusion proteins containing DsRed variants (including mCherry). Western blot analysis using lysates from HEK 293 cells stably expressing DsRed-express revealed a single band of 30–38 kDa. No band in this molecular weight range was seen in Westerns from lysates of untransfected cells or from cells expressing AcGFP1 (manufacturer's information). No labeling was seen in brains from mice without r-AAV5 injections.

In situ hybridization

To determine the distribution of C1 (PNMT + TH) and A1 (TH only) neurons in mouse medulla oblongata, three mice were anesthetized and perfused transcardially with 3 % paraformaldehyde. Brains were removed and postfixed in the same fixative for 16−18 h at 4 °C. Brains were sectioned and placed in cryoprotectant as described above. Sections were briefly washed in sterile phosphate buffered saline, mounted on charged slides and dried overnight. After 2 rinses in sterile water, sections were incubated with "pretreat 4" from the RNAscope Multiplex Fluorescent Assay kit (Advanced Cell Diagnostics, Hayward, CA, USA) for 30 min at 42 °C. Sections were rinsed twice in sterile water and incubated in RNAscope catalog

oligonucleotide probes for PNMT and TH for 2 h at 42 °C. PNMT probes were based on the sequence for mouse PNMT (NM_008890.1) spanning base pairs 2-849. TH probes were based on the sequence for mouse TH (NM_009377.1) spanning base pairs 483-2603. PNMT was used in RNAscope channel 1 and TH in channel 2. After incubation in probes, tissue was treated exactly according to the manufacturer's protocol (ACD) using Amp 4 Alt A-FL in the final incubation resulting in PNMT transcripts being tagged with Alexa 488 and TH transcripts with Atto 550. Slides were covered with Prolong Diamond Antifade mountant (Molecular Probes, Eugene, OR, USA).

Mapping

A one in three series of 30 μm transverse sections through the brain were examined for each experiment under bright field and epifluorescence using a Zeiss AxioImager Z.1 microscope (Carl Zeiss Microimaging, Thornwood, NY, USA). Either horizontal or transverse spinal cord sections were sampled from all levels within cervical, thoracic and lumbar cord. Neurons immunoreactive for TH, EGFP, and/ or mCherry were plotted with the Neurolucida software (Micro Brightfield, Colchester, VT, USA) utilizing a Ludl motor-driven microscope stage and the Zeiss MRC camera, after methods previously described (Stornetta et al. 2004). Filter settings for the Cy3 or Atto 550, Alexa 488 and Dylight 649 fluorophores were as follows: Alexa 488, excitation of 500 nm, emission of 535 nm; Cy3/Atto 550, excitation of 545, emission of 605 nm; Dylight 649, excitation of 640 nm, emission of 690 nm. Only cell profiles that included a nucleus were counted and/or mapped except in the cases where collaterals were mapped. The Neurolucida files were exported into the Canvas drawing software (Version 10, ACD Systems, Inc.) for text labeling and final presentation. The neuroanatomical nomenclature is after Paxinos and Franklin (2013). Photographs were taken with a Zeiss MRC camera (resolution 1388 × 1040 pixels) and the resulting TIFF files were imported into the Canvas software. Output levels were adjusted to include all information-containing pixels. Balance and contrast was adjusted to reflect true rendering as much as possible. No other "photo-retouching" was done. Figures were assembled and labeled within the Canvas software.

Results

All cases are summarized in Table 1. There was no correlation between the titer of rabies-EGFP and the number of starter cells or first-order projecting neurons (Pearson's $r = 0.227$, $p = 0.255$) although there was a strong correlation between the number of starter cells and the number

of first-order projecting neurons as would be expected (Pearson's $r = 0.684$, $p = 0.00008$).

TVA-mCherry expression is restricted to catecholamine neurons in ventrolateral medulla

TVA-mCherry was expressed almost exclusively by TH-immunoreactive (ir) cells within the ventrolateral medulla (VLM) ($N = 16$ mice; 95 ± 0.9 % of TVA-mCherry labeled neurons were TH-ir) (Fig. 1).

No "helper vectors" control In 2 mice (cases 32 and 34), neither FLEX-TVA nor FLEX-RG was injected into the medulla, although rabies vector was injected into the hypothalamus. No rabies-EGFP labeled cells were detected in the brainstem of these animals.

No FLEX-RG control In 6 mice, the FLEX-TVA was injected without FLEX-RG. Rabies vector was later injected into hypothalamus (cases 32, 34, 57) or spinal cord (cases 58, 59, 60). In the hypothalamic injected mice, 1 "starter cell" (Rabies-EGFP + TVA-mCherry in the VLM) was found in 2 of the mice and 9 were found in the other mouse (see example of starter cell in Fig. 2). In the spinal cord-injected mice, 0, 1 or 2 starter cells were found in the VLM. There was no evidence of trans-synaptic transport of rabies in any of the spinal cord and in two of the hypothalamus cases, i.e., no EGFP was detected in non-TVA-mCherry labeled cells. However, in the hypothalamus case with 9 starter cells, there were 5 rabies-EGFP neurons with no TVA-mCherry in the brainstem indicating some "leak" of non-RG dependent rabies virus from starter cells in this case. (Note: all cell counts were based on a one in three series of 30 μm sections.)

Cases with rabies vector injected into the upper thoracic spinal cord In 4 mice (cases 48, 53,54,55) rabies was injected into the T2–T3 segments of the spinal cord 6 weeks following left side injections of FLEX-TVA and FLEX-RG into the C1 area of the RVLM. After 10 days, all neurons labeled for TVA were located on the left side and 114 ± 25.5 out of 195 ± 11.8 TH neurons (57 ± 11.4 %) were labeled for TVA. These counts were made in a 1 in 3 series of 30 μm sections for a total of 12 sections between coronal sections inclusive of 7.19–6.35 mm caudal to bregma. An average of 12.8 ± 4.5 bulbospinal starter cells (TVA+/EGFP+) were observed in the RVLM (Fig. 3; filled red squares). The location of these neurons within the RVLM was similar to that of spinally projecting C1 neurons in rats (Dun et al. 2002; Sawchenko and Bohn 1989; Tucker et al. 1987; Ross et al. 1981) and mice (VanderHorst and Ulfhake 2006); specifically these neurons were confined to the rostral end of the VLM.

The axonal collaterals of the bulbospinal C1 starter cells were identified by the dual presence of TVA-mCherry and

Table 1 All cases examined

Case	Rabies-EGFP injection	Titer of rabies-EGFP (tu/ml)	Total TH (1 in 3 series)	TVA + TH (1 in 3 series)	Starter cells (1 in 3 series)	First order cells (1 in 3 series)
20	Hypothalamus	4.3×10^8			20	234
21	Hypothalamus	4.3×10^8			13	75
22	Hypothalamus	4.3×10^8			28	150
32 (no RG)	Hypothalamus	4.3×10^8			1	0
33	Hypothalamus	3.6×10^7			2	0
34 (no RG)	Hypothalamus	4.3×10^8			8	0
35	Hypothalamus	3.6×10^7			3	1
36	Hypothalamus	1.1×10^8			4	18
37	Hypothalamus	1.1×10^8			0	0
38	Hypothalamus	1.1×10^8	255	131	25	202
39 (no TVA or RG)	Hypothalamus	1.1×10^8			0	0
40 (no TVA or RG)	Hypothalamus	1.1×10^8			0	0
41	Hypothalamus	1.1×10^8			7	25
42	Hypothalamus	1.1×10^8			47	108
43	Hypothalamus	1.1×10^8			1	22
44	Hypothalamus	1.1×10^8			5	6
48	Spinal cord	1.1×10^8	190	126	7	34
49	Hypothalamus	3.0×10^7	173	107	8	98
50	Hypothalamus	3.0×10^7	174	68	9	9
52	Hypothalamus	3.0×10^7	190	100	12	13
53	Spinal cord	1.1×10^8	226	150	20	34
54	Spinal cord	1.1×10^8			11	7
55	Spinal cord	1.1×10^8	195	141	21	26
57 (no RG)	Hypothalamus	1.1×10^8			9	5
58 (no RG)	Spinal cord	1.1×10^8			0	0
59 (no RG)	Spinal cord	1.1×10^8			1	0
60 (no RG)	Spinal cord	1.1×10^8	169	39	3	0

rabies-EGFP fluorescence (see Fig. 4a–c, g–i). This method allowed us to examine the collaterals of the starter cells regardless of whether or not the Flexed-RG vector had been injected into the RVLM. Although we used a spinal cord case that had no RG injection and no first-order neurons (Case #60) for the drawings, we nonetheless verified the double-labeling for all collaterals drawn from a series of transverse sections from brainstem through midbrain and illustrated in Fig. 5a, c. Projection fields were identified in the nucleus of the solitary tract, the A1 cell group, the dorsal motor nucleus of the vagus, C1 cell group, raphe pallidus, raphe magnus, locus coeruleus, lateral parabrachial nucleus, and ventrolateral periaqueductal gray. The bulbospinal C1 neurons had no terminal fields rostral to the midbrain. The afferents to the starter cells were identified as rabies-EGFP-expressing neurons devoid of TVA-mCherry. An example of a first-order neuron from a spinal cord injected case is illustrated in Fig. 6a, b. The

rabies-EGFP typically filled all cell processes, including dendrites, axons and terminals. The four cases had an average of 25.3 ± 6.4 first-order projecting neurons counted in a one in three series of 30 μm sections. The distribution of these first-order projecting neurons for the four spinal cord injected cases are collated onto representative sections and illustrated in Fig. 7 (neurons are depicted as filled red or black circles). Most first-order projecting neurons were located within the reticular formation throughout the brainstem/pons and were also present more sparsely in the more caudal portions of the spinal trigeminal nucleus, the nucleus of the solitary tract, caudal ventrolateral medulla, the cerebellum, lateral parabrachial nucleus, deep layers of inferior/superior colliculus and periaqueductal gray. A few neurons were located in the lateral hypothalamus (not illustrated).

Cases with rabies vector injected into the hypothalamus Rabies vector was injected in hypothalamus of 14 mice

Fig. 1 TVA-mCherry is expressed selectively in catecholamine neurons in the ventrolateral medulla. Examples of neurons expressing TVA-mCherry (**a**) that also express tyrosine hydroxylase (TH)-immunoreactivity (**b**). These neurons are distributed throughout the ventrolateral medulla as indicated in **c** for 4 cases with rabies-EGFP injected in the spinal cord (*open circles*) and 11 cases with rabies-EGFP injected in hypothalamus (*open triangles*) with the average of all cases indicated by *open squares*. *Scale* in **a** 20 μm
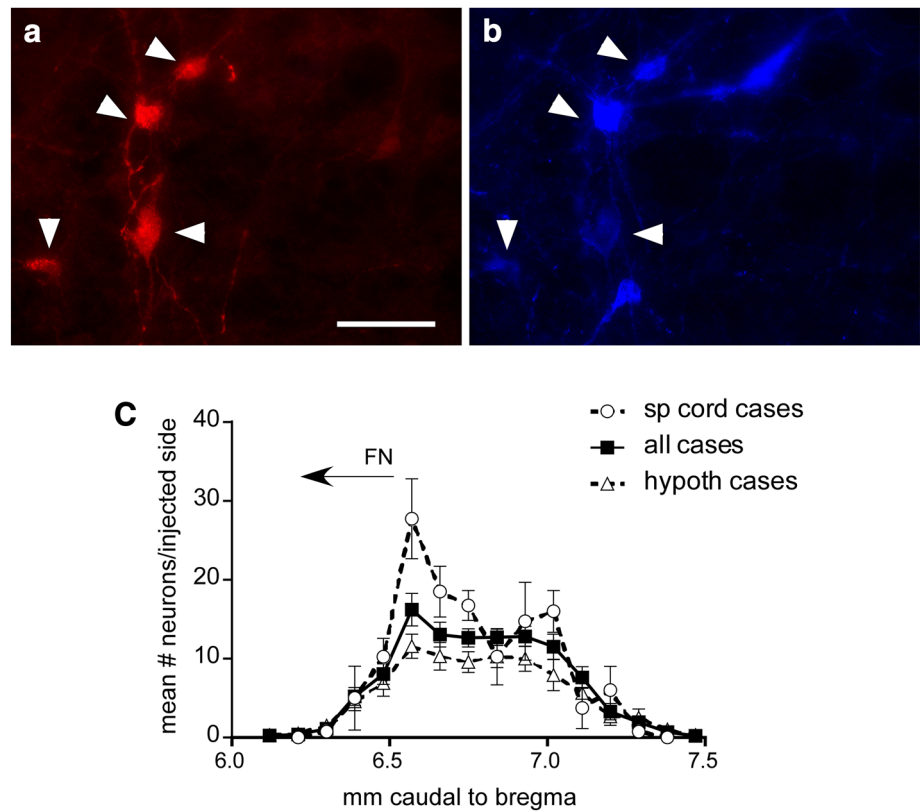
Fig. 2 Example of starter cell. TVA-mCherry expressing neuron indicated by an asterisk (**a**) containing TH-immunoreactivity (**b**) and retrogradely labeled from the spinal cord with rabies-EGFP (**c**). The merged image is shown in **d**. *Scale* in **d** 25 μm
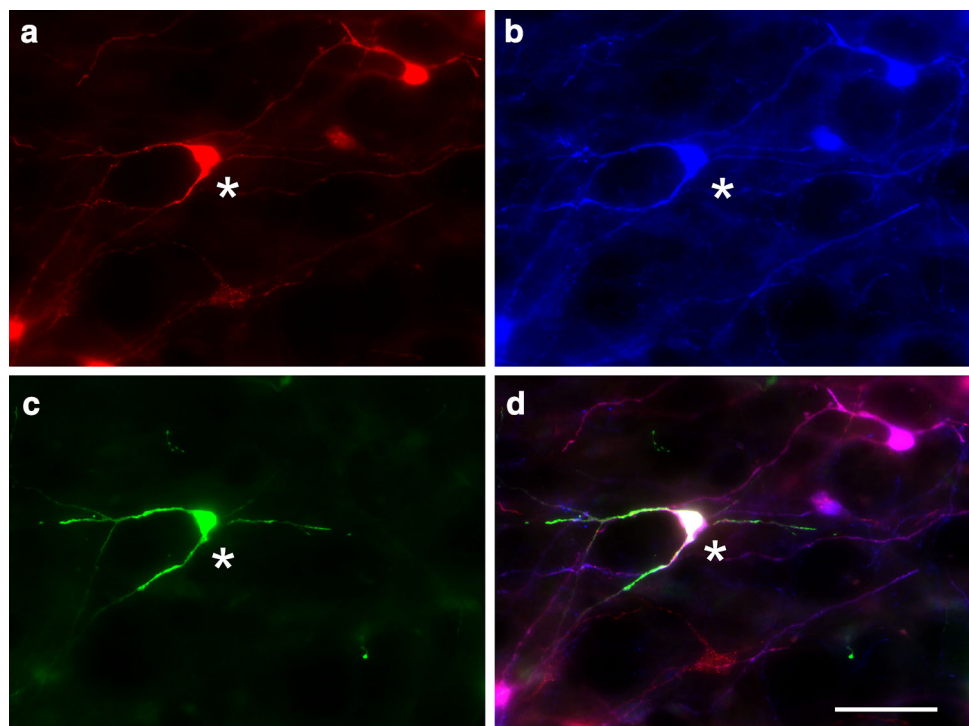
Fig. 3 Starter cells are distributed in overlapping but slightly different levels in ventrolateral medulla depending on hypothalamic or spinal cord injection of rabies virus. Drawings of representative coronal sections throughout the medulla oblongata showing the composite location of starter cells from 4 cases with rabies-EGFP injected in hypothalamus (*yellow circles*) and 4 cases with rabies-EGFP injected in spinal cord (*red squares*). Approximate location of coronal section in mm caudal to bregma indicated in lower left corner of each section. *Scale* 1 mm. *4V* fourth ventricle, *7* facial motor nucleus, *10* dorsal vagal complex, *12* hypoglossal nucleus, *Amb* ambiguus nucleus, *Cb* cerebellum, *DC* dorsal cochlear nucleus, *icp* inferior cerebellar peduncle, *IO* inferior olivary nucleus, *py* pyramidal tract, *sp5* spinal trigeminal tract, *Sol* nucleus of the solitary tract, *st* solitary tract
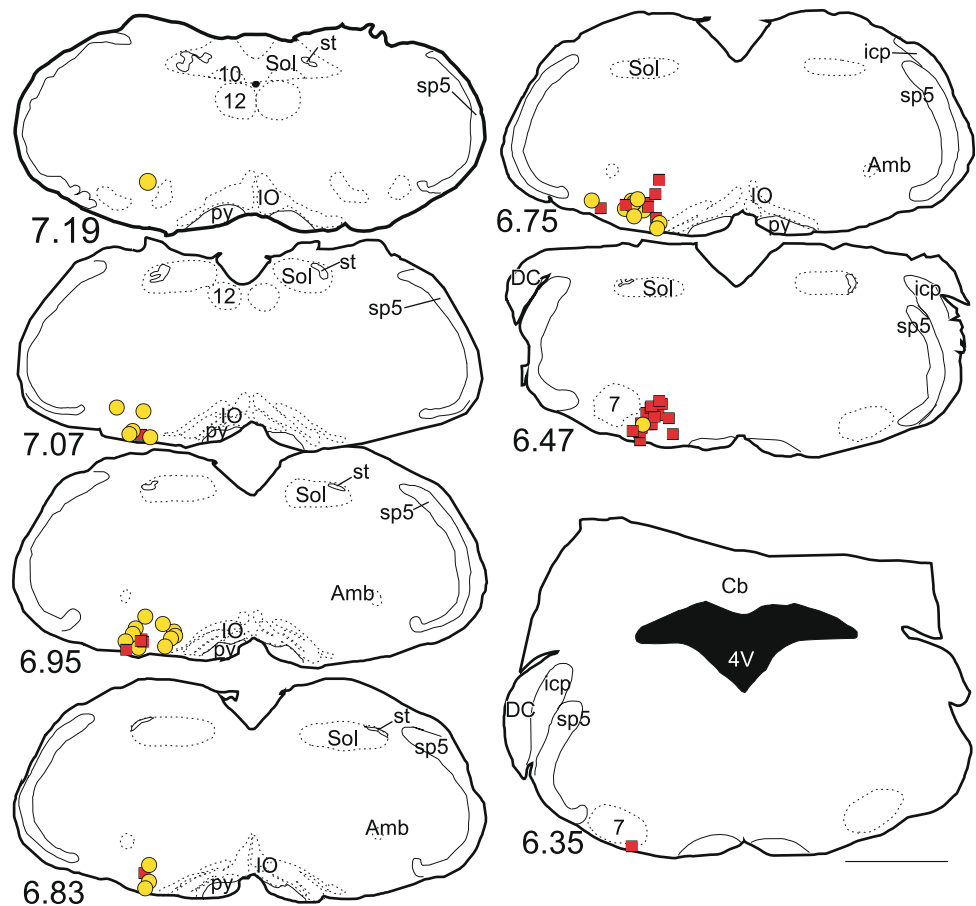
4–6 weeks following injections of FLEX-TVA and FLEX-RG into the left C1 area of the RVLM. After 10 days, animals were euthanized and brains collected. In one case (Case #37), no EGFP-labeled cells were observed in brainstem. In the remaining 13 cases, we observed starter cells in ventrolateral medulla and first-order (EGFP-only) cells distributed throughout the brainstem/pons and midbrain. Four of these cases (Cases #38, 49, 50, 52) were selected for more extensive study because they had approximately the same number of starter cells (13.5 ± 3.9, counted in a one in three series of 30 μm sections in a total of 12 sections spanning 7.19–6.35 mm caudal to bregma) as the four spinal cord cases just described. On the left side of the brain, which contained all TVA+ neurons, 101.5 ± 13.0 out of 198 ± 19.4 (51.2 ± 4.7 %) TH+ neurons were TVA+. The rabies virus injection sites for these four cases are illustrated in Fig. 8.

The starter TH-ir cells from these four cases represented as yellow circles (or light gray in black and white) in Fig. 3 were located more caudally in the VLM than those observed after spinal injection of rabies-EGFP represented as red (or black in black and white) squares in Fig. 3 and may have included a few A1 neurons based on the

distribution of PNMT-immunoreactive neurons in mice (Holloway et al. 2013) and the distribution of PNMT and TH transcripts (see below). This observation is consistent with prior work in rats which showed that C1 cells with hypothalamic projection are located more caudally than those with spinal projections (Verberne et al. 1999; Stornetta et al. 1999; Tucker et al. 1987).

Hypothalamus-projecting starter cells had rabies-EGFP and TVA-mCherry fluorescence throughout their dendrites, axons and synaptic boutons (examples in Fig. 4d–f, h–j). This double labeling was verified for all projections depicted in Fig. 5b, d. Case #57 was used for this drawing (the case with 9 starter cells with no FLEX-RG described in the Controls section above). Terminal fields of hypothalamus-projecting C1 cells were located in the same brain regions as those of the spinally projecting ones. The projections appear more extensive in this case than that shown for the spinal cord case due to the greater number of starter cells (9 starter cells in hypothalamus case vs. 3 starter cells in the spinal cord case). Starter cell collaterals were also verified in the other 4 hypothalamus cases with starter cells depicted in Fig. 3. In all cases, collateral terminal fields were observed in the following regions: the A1 cell group, the nucleus of the solitary tract, the dorsal motor
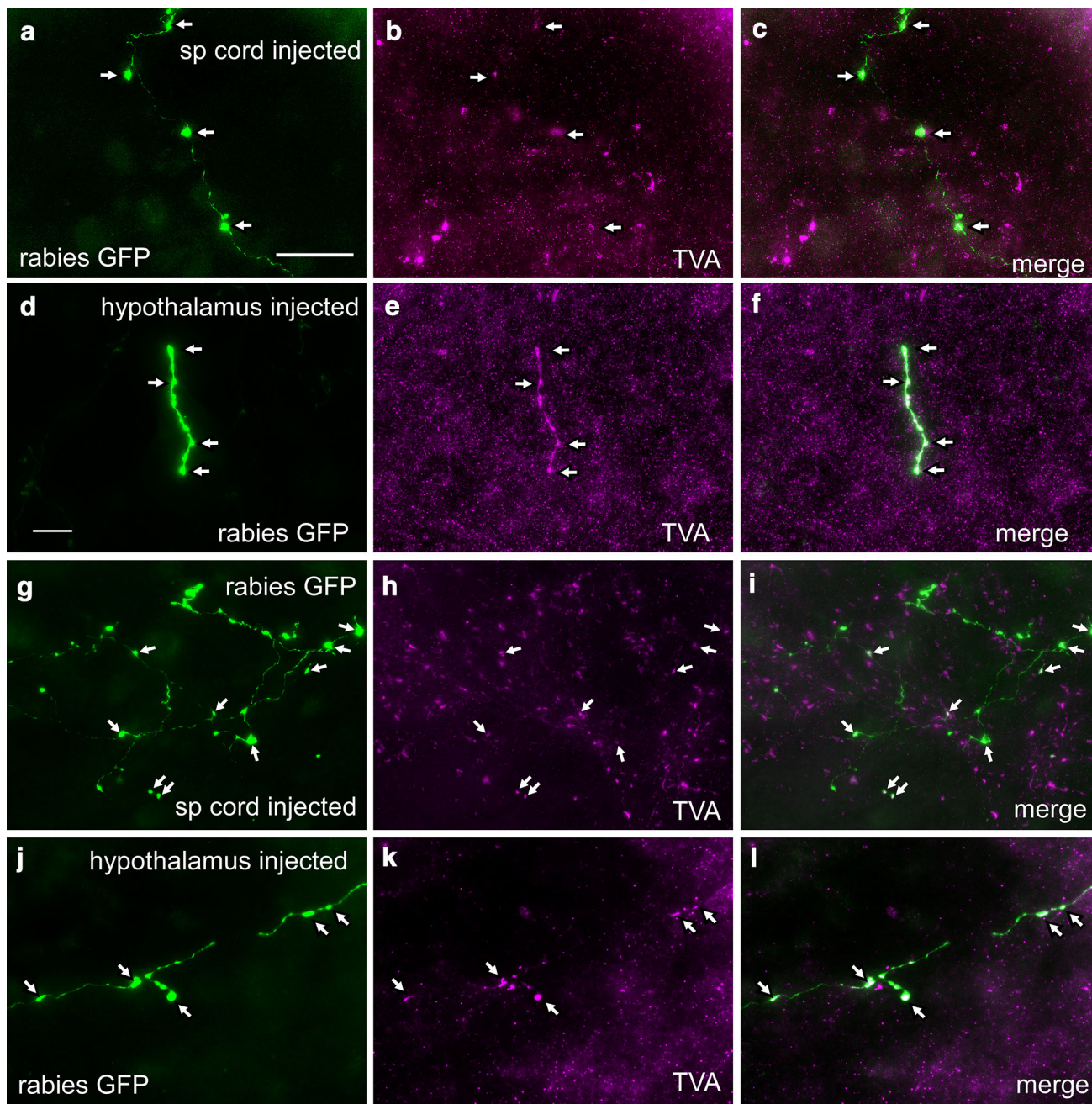
Fig. 4 Examples of terminal fields from starter cells in cases with rabies-EGFP injected in either the spinal cord or hypothalamus. **a–c** Terminal field in the locus coeruleus from a case with rabies-EGFP injected in the spinal cord. **d–f** Terminal field in the locus coeruleus from a case with rabies-EGFP injected in the hypothalamus. *Arrows* point to bouton-like structures in all panels. **g–i** Terminal field in the dorsal motor nucleus of the vagus from a case with rabies-EGFP injected in the spinal cord. **j–l** Terminal field in the dorsal motor nucleus of the vagus from a case with rabies-EGFP injected in the hypothalamus. *Scale* in **a** 20 μm for all panels

nucleus of the vagus, C1 cell group, raphe pallidus, raphe magnus, locus coeruleus, and ventrolateral periaqueductal gray. We noted no discernible rabies-EGFP terminals also labeled with TVA in the lateral parabrachial nucleus in any of the hypothalamus cases examined, whereas in 4 spinal cord cases (Cases # 48, 53, 55, 60) this nucleus did have double-labeled terminals.

First-order projecting neurons (examples in Fig. 6c, d) from four cases with rabies-EGFP injected in the hypothalamus are collated onto representative transverse sections (Fig. 7, yellow or light gray filled circles). These neurons were found in similar areas as those from spinal cord cases, although extending a bit more caudally in the reticular formation and nucleus of the solitary tract. First-
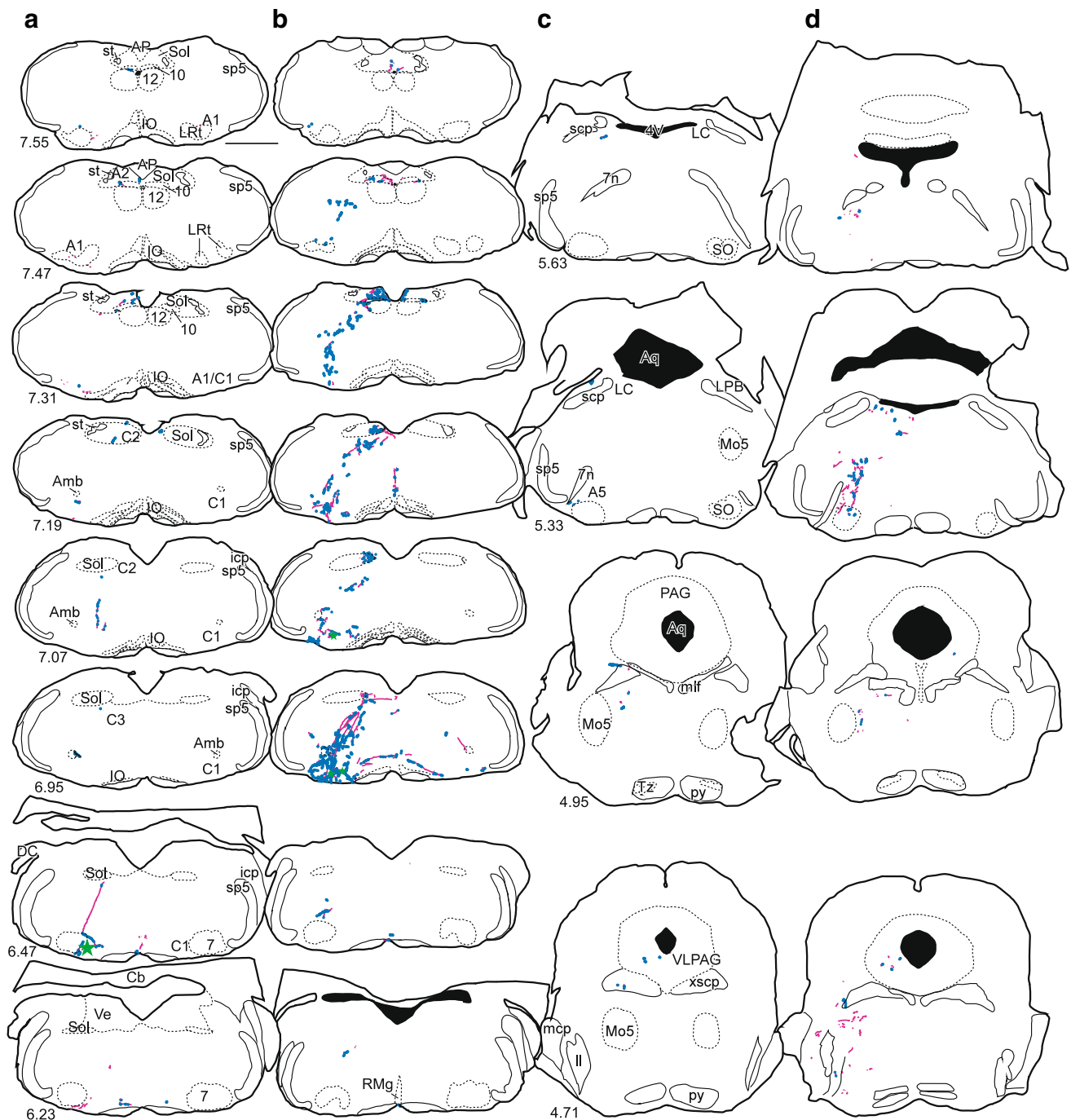
Fig. 5 Starter cells retrogradely labeled from either hypothalamus or spinal cord have collateral projections to similar regions. Drawings of representative coronal sections showing starter cells (*green stars*) and collaterals (*pink lines*) and bouton-like structures (*blue dots*) from a case injected with rabies-EGFP in the spinal cord (columns **a** and **c**) and a case with rabies-EGFP injected in the hypothalamus (columns **b** and **d**). *Numbers* in the lower left corner of sections in **a**, **c** refer to the location of the sections in mm caudal to bregma and also pertain to the adjacent section in columns **b** and **d**. *Scale bar* is 1 mm. Abbreviations as in Fig. 3 with following additional abbreviations: *7n*

facial nerve, *AP* area postrema, *Aq* aqueduct, *A1* A1 noradrenergic cell group, *A1/C1* A1/C1 catecholaminergic cell group, *A5* A5 catecholaminergic group, *C1* C1 adrenergic cell group, *C2* C2 adrenergic cell group, *C3* C3 adrenergic cell group, *LPB* lateral parabrachial nucleus, *LC* locus coeruleus, *mcp* middle cerebellar peduncle, *mlf* medial longitudinal fasciculus, *Mo5* motor trigeminal nucleus, *RMg* raphe magnus, *scp* superior cerebellar peduncle, *SO* superior olivary nucleus, *Tz* nucleus of the trapezoid body, *VLPAG* ventrolateral periaqueductal gray, *xscp* decussation of the superior cerebellar peduncle

Fig. 6 Examples of first-order projecting neurons from cases injected with rabies-EGFP. **a, b** First-order projecting neuron located in the inferior colliculus from case injected with rabies-EGFP in spinal cord. **c, d** First-order projecting neurons located in the nucleus of the solitary tract from case injected with rabies-EGFP in the hypothalamus. **e** First-order projecting neurons located in deep layers of the cervical spinal cord dorsal horn from case injected with rabies-EGFP in hypothalamus. *Scale* in **a** 200 μm for **a**; 50 μm for **b, d**; 100 μm for **c, e**
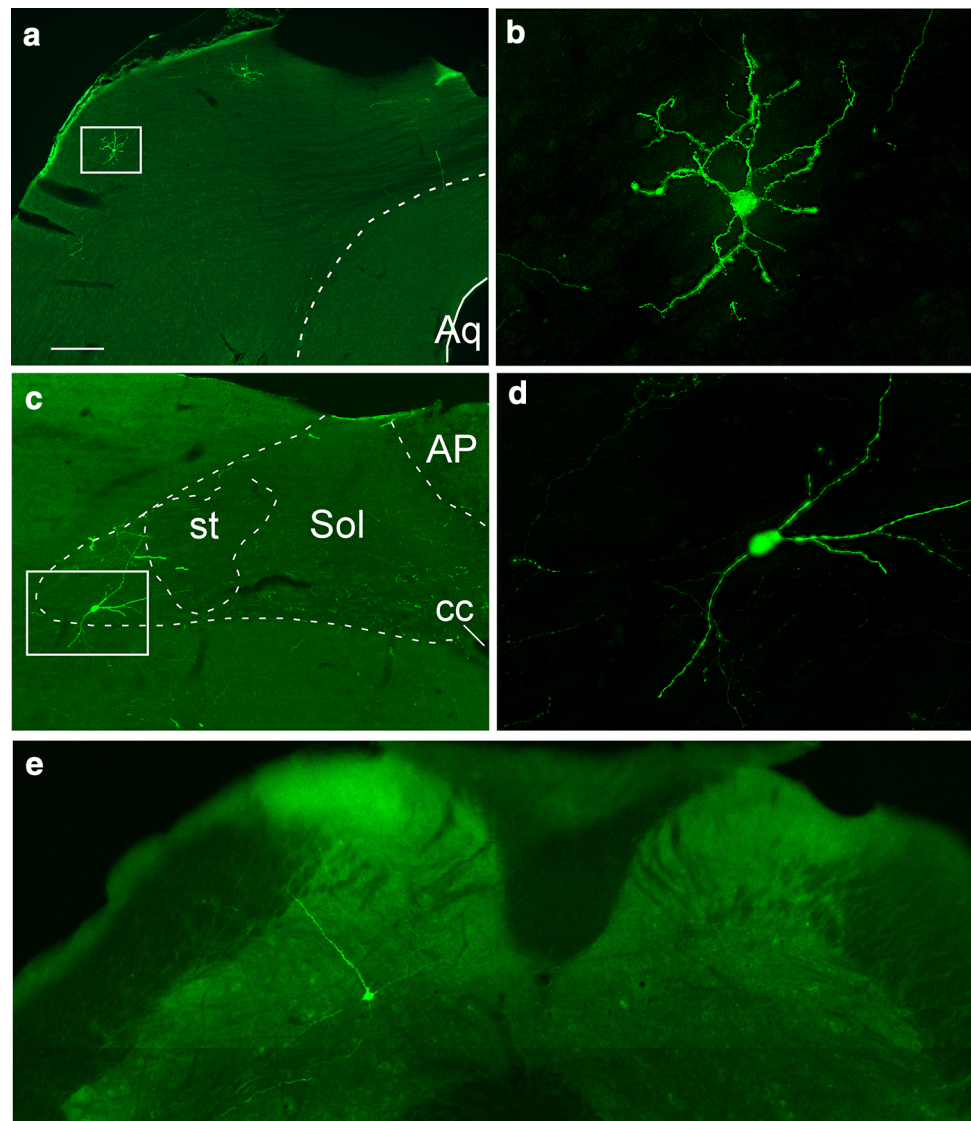
order neurons were present in relative abundance in the reticular formation throughout the medulla/pons and were also located in caudal portions of the spinal trigeminal nucleus, the nucleus of the solitary tract, caudal ventro-lateral medulla, the cerebellum, lateral parabrachial nucleus, more superficial as well as deep layers of infe-rior/superior colliculus and periaqueductal gray. One first-order projecting neuron was found in the deep layers of the dorsal horn of the cervical spinal cord in one case (Fig. 6e).

In four cases, there were EGFP-labeled neurons in the same plane as the injection site in hypothalamus; we speculate that these neurons were injured by the injection pipette and were directly labeled with rabies virus as they seemed to follow the injection track. Unfortunately, this artifact prevents us from making a definitive statement about first-order projecting neurons in the hypothalamus of these cases.

In 2 cases each of either hypothalamus or spinal cord-targeted injections of rabies-EGFP, we observed a total of 4 first-order catecholaminergic neurons (e.g., rabies-EGFP and TH-positive but TVA-mCherry-negative) located in the C1 and C3 areas as well as in the A5 region (not illustrated).

Distribution of A1 and C1 neurons in mouse

An example of neurons expressing TH and PNMT mRNA visualized with the RNAscope method for ISH is illustrated in Fig. 9a, b. The distribution of these neurons throughout the medulla oblongata is shown in a series of transverse sections from caudal to rostral in Fig. 9c. A1 neurons (with only TH transcripts) were found from the decussation of the pyramids to just rostral to the point where the lateral reticular nucleus separates into two lobes ($\sim$7.31 mm
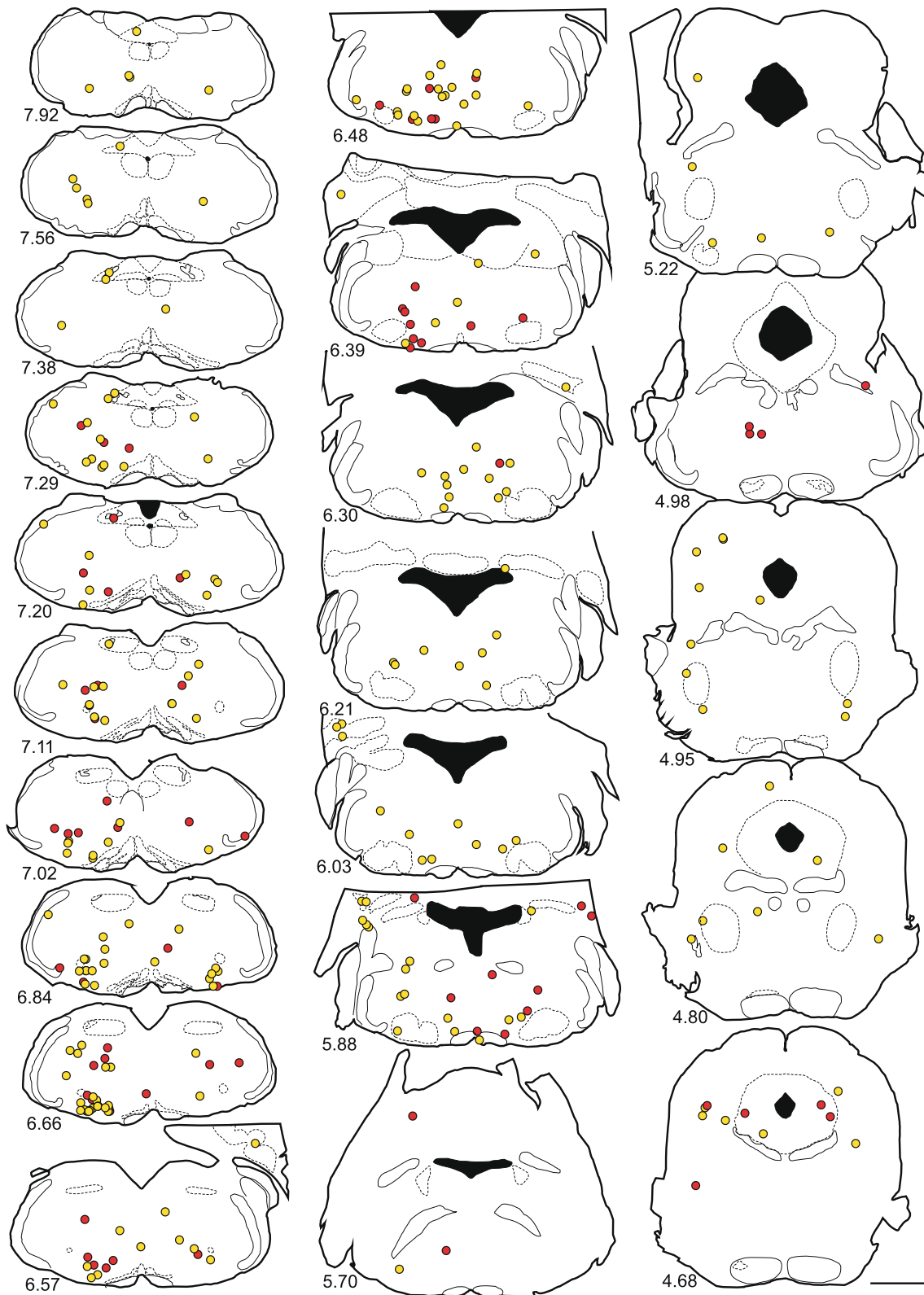
Fig. 7 First-order projecting neurons are distributed in overlapping areas throughout brainstem/pons and midbrain regardless of hypothalamic or spinal cord injection of rabies virus. Drawings of representative coronal sections throughout the brainstem/pons/midbrain showing the composite location of first-order projecting neurons from 4 cases with rabies-EGFP injected in hypothalamus (*yellow circles*) and 4 cases with rabies-EGFP injected in spinal cord (*red circles*). These are from the same cases depicted in Fig. 3. Approximate location of coronal section in mm caudal to bregma indicated in lower left corner of each section. *Scale bar* 1 mm
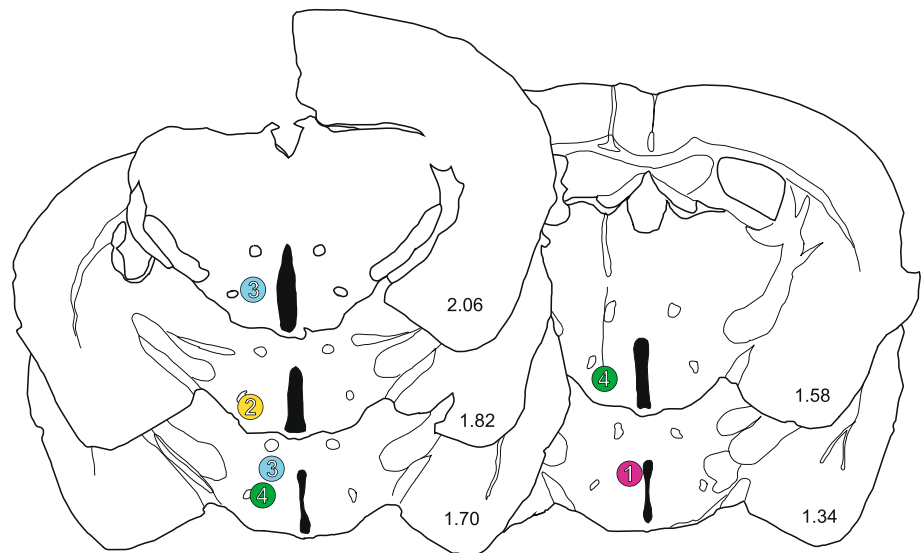
caudal to bregma) although a few scattered A1 neurons (PNMT-TH+) could be observed as far rostral as the level of the linear nucleus (~7.07 mm caudal to bregma). TH+ neurons without PNMT mRNA were also observed in more rostral sections beginning about 6.59 mm caudal to bregma. These neurons likely belong to the A5 cell group. Neurons containing both TH and PNMT transcripts (C1 neurons) were located in the ventrolateral medulla between ~7.07 and 6.35 mm caudal to bregma.

Discussion

We describe the axonal projection fields and putative monosynaptic inputs of spinally projecting and forebrain-projecting C1 neurons of the mouse using a modified rabies virus in combination with a DβH-Cre transgenic mouse model. Our first conclusion is that, regardless of whether the C1 cells innervate the cord or the hypothalamus, these neurons also target a common set of ponto-medullary and midbrain regions, depicted schematically in Fig. 10. Secondly, these two subsets of C1 cells receive input from the same general brain regions, summarized in Fig. 11. In short, the C1 cells are even more highly collateralized than previously thought and they may have a number of common inputs regardless of whether they innervate the spinal cord or the hypothalamus.

Caveats

The modified rabies virus approach has limitations such as potential expression of TVA by non-Cre-expressing neurons (Callaway and Luo 2015). Although we did not use

the more stringent form of TVA (TVA66T) described by Callaway and Luo (2015), 95 % of the TVA-expressing neurons contained tyrosine hydroxylase such that our starter cells were by and large the C1 neurons of the ventrolateral medulla. We also observed that a majority of the C1 neurons (~54 %) expressed the TVA in the 8 cases we analyzed more extensively, allowing a reasonable representation of C1 terminals for the entry of rabies into projection fields in spinal cord and hypothalamus.

As has been the case with other experiments using this method, we observed a rather sparse set of connecting first order neurons (Callaway and Luo 2015). We presume that these first-order neurons were correctly identified based on previous reports using the same method to elucidate synaptic connections elsewhere in the brain (Wall et al. 2010; Weible et al. 2010; Wickersham et al. 2007a, b; Callaway and Luo 2015). However, we did not detect any input from several previously reported sources of probable afferents to the C1 cells such as the locus coeruleus (Card et al. 2011), vestibular nucleus (Holstein et al. 2011, 2014), and the superficial laminae of the spinal cord (Westlund and Craig 1996). This could be due to a number of factors, including the absence of RG receptors (nicotinic acetylcholine receptors and NCAMs; Lafon 2005) on the nerve terminals of these afferent neurons. Another factor affecting the number of connecting first order neurons is the rather small number of starter cells we obtained (~12 % of the TVA+ TH+ neurons or 6.7 % of total TH neurons of the C1 region on one side of the brain).

Conceivably, the rabies-EGFP method we used selected for a small subset of C1 neurons (~10 % in the rat, Stornetta et al. 1999) that project to both hypothalamus and spinal cord as perhaps these more widely collateralized
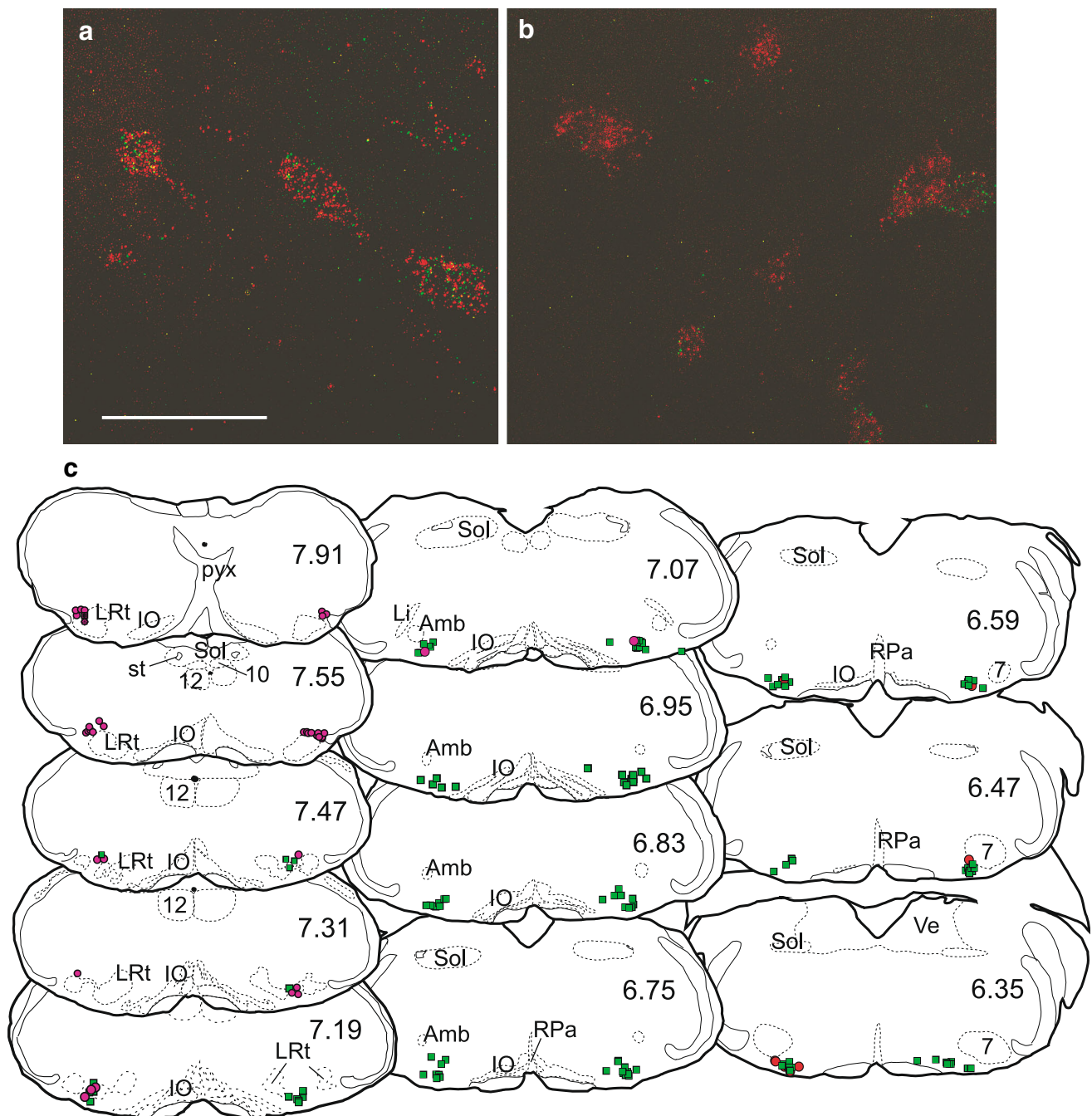
Fig. 9 Relative location of A1 and C1 neurons in mouse brain. Photomicrographs of TH and phenylethanolamine n-methyltransferase (PNMT) mRNA in ventrolateral medulla visualized with RNAscope at **a** 6.47 mm or **b** 7.3 mm caudal to bregma. PNMT transcripts are tagged with Alexa 488 and appear as *green dots*. TH transcripts are tagged with Atto 550 and appear as *red dots*. *Scale* in **a** = 50 μm for **a**, **b** and ∼ 2 mm for **c**. The distribution of neurons containing TH mRNA only (*magenta circles* representing A1 or *red circles* representing A5) or both TH and PNMT transcripts (*green squares*) is shown in (**c**). Approximate location of coronal section in mm caudal to bregma indicated in right corner of each section. *Li* linear nucleus; other abbreviations as above

neurons have a higher density of terminal synaptic contacts and thus might more readily take up rabies-EGFP (Callaway and Luo 2015). We are also unable to make a definitive conclusion regarding the absolute number of

neurons that contact the C1 cells synaptically because differing numbers of synaptic connections or subcellular localization of the RG receptor may influence the spread of the rabies-EGFP (Callaway and Luo 2015). Although our
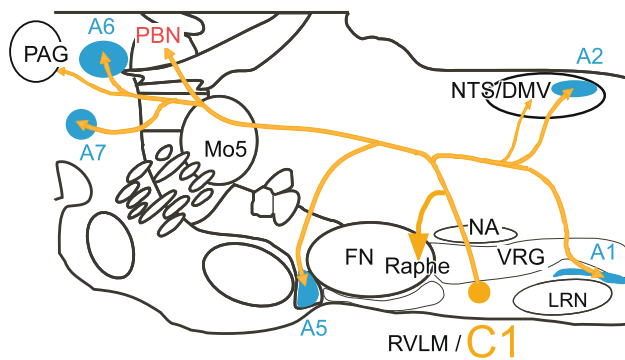
Fig. 10 Summary figure showing projections of C1 neurons. PBN is indicated in *red* as we only found evidence for collaterals from bulbospinal C1 neurons. Noradrenergic clusters indicated in *blue*

main conclusion is that both forebrain and spinal cord projecting C1 neurons have a common set of neuronal afferents and targets (see Figs. 10, 11), our data can only support this hypothesis in terms of general brain regions. Bulbospinal and hypothalamic-projecting C1 cells could conceivably target completely different sets of neurons within the same general regions of the brain. For example, in the dorsal motor vagal complex, motor neurons projecting to the fundus and antrum are intermixed (Pearson et al. 2007).

Our experiments with injections of TVA without RG resulted in much fewer starter neurons than in experiments that included RG. These results support the idea that RG might participate in the retrograde axonal transport of the rabies virus by enhancing binding to either NCAM or p75 nerve growth factor receptor (Gluska et al. 2014) and accelerating the rate/efficiency of axonal transport.

We refer to the starter cells as C1 neurons, implying that these catecholaminergic neurons express both phenylethanolamine-N-methyl transferase (PNMT) and TH. We did not verify that the TVA neurons express PNMT but we verified that, within the region that harbored starter cells, most neurons contained both TH and PNMT mRNA. This

same region contains almost exclusively PNMT-immunoreactive neurons in mice (Holloway et al. 2013).

Collaterals of C1 neurons with forebrain vs. spinal cord projection

The global projections of the C1 neurons have been previously described in rats (Card et al. 2006) and mice (Abbott et al. 2013) using vector-based anterograde tracers. Our results agree with these reports and other reports detailing subsets of C1 projections in rats including, e.g., to the dorsal motor nucleus of the vagus (Pickel et al. 1986) (note Ruggiero found C1 with collaterals to spinal cord project to DMV/NTS, Mtui et al. 1995), the NTS (Rukhadze and Kubin 2007), raphe pallidus (Luppi et al. 1989), the PAG (Clement et al. 1998; Herbert and Saper 1992), locus coeruleus (Milner et al. 1989; Holloway et al. 2013), A1 (Holloway et al. 2013), and local connections within the C1 area (Agassandian et al. 2012). We also noted that both subsets of C1 neurons targeted all the other catecholaminergic cell groups in medulla/pons (A1, A2, C1, C2, C3, A5, A6). We were unable to detect any differences in the projection areas within the medulla oblongata/pons/midbrain of the collaterals of spinal vs. forebrain-projecting C1 neurons with the possible exception of the lateral parabrachial nucleus, which was only contacted by bulbospinal C1 neurons. The sympathetic preganglionic neurons in spinal cord are topographically distributed with regard to specific outputs (Pyner and Coote 1994) and several authors would argue for regionally specific outputs of C1 neurons (Dampney and McAllen 1988; McAllen and Dampney 1990; Mueller et al. 2011). However, using the pseudorabies method, the same C1 neuron can be labeled from multiple targets (e.g., stellate and adrenal, Jansen et al. 1995), implying that a given C1 neuron can project to different sets of sympathetic preganglionic neurons. In the current study, we could not discriminate specific target areas of either spinal cord or hypothalamus-projecting C1 neurons, except for the

Fig. 11 Summary figure showing location of first-order projection neurons to C1 neurons
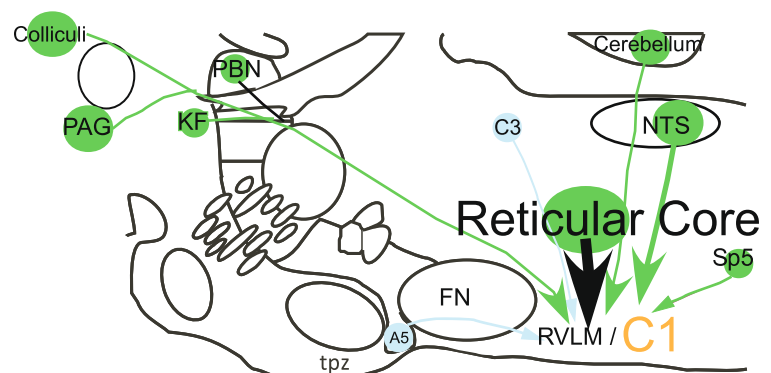
aforementioned lateral parabrachial nucleus. It is possible that C1 neurons share the same outputs regardless of whether they have spinal or hypothalamic collaterals. To examine whether specific subsets of C1 neurons target different outputs, a more specific labeling of the subsets of sympathetic preganglionic neurons or of specific neurons in the hypothalamus by rabies-EGFP would be required. Another approach would be to determine whether the C1 collaterals are contacting specific phenotypes in target areas, e.g., do C1 neurons with hypothalamic vs. spinal collaterals contact DMV motor neurons projecting to pancreas vs. heart. It is also possible that the varying physiological responses elicited from C1 neurons could be accounted for by their spinal vs. hypothalamic targets.

First-order projecting neurons

Projections to the rostral ventrolateral medulla at large have been described previously from many of the areas where we observed first-order projecting neurons. There is ultrastructural evidence of monosynaptic inputs to the C1 cells from the NTS (Aicher et al. 1996) and from the orexinergic neurons (Puskas et al. 2010); we observed first-order projecting neurons in both of these areas. Other areas with first-order projecting neurons in line with previous reports include the caudal spinal trigeminal nucleus (Esser et al. 1998), the PAG (Chan and Sawchenko 1995; Van Bockstaele et al. 1991; Farkas et al. 1998; Sartor and Verberne 2003), the raphe (Nicholas and Hancock 1990), the CVLM (Chan and Sawchenko 1998; Schreihofer and Guyenet 2002), and the PBN (Saper and Loewy 1980).

The first-order projecting neurons seen in the cerebellum near the fastigial nucleus could be mediating the pressor response elicited by stimulating this nucleus (McAllen 1985). The somato-sympathetic reflex, known to relay through the ventrolateral medulla (Zanzinger et al. 1994; Stornetta et al. 1989; McAllen 1985; Miyawaki et al. 2002) could be mediated by first-order neurons projecting to the C1 neurons seen in the caudal spinal trigeminal nucleus or the deep layers of the dorsal horn of the spinal cord and/or the reticular core. The respiratory modulation of the C1 neurons could also originate from respiratory-related neurons in the reticular core (Haselton and Guyenet 1989a, b). The first-order neurons in the superficial and deep layers of inferior and superior colliculus may mediate the autonomic response to sudden visual or acoustic stimuli (Muller-Ribeiro et al. 2014). Stimulation of sites in ventrolateral PAG in the same area where we report first-order projecting neurons can modulate responses in RVLM neurons (Lovick 1992a, b). The ventrolateral PAG has also been shown to project to the RVLM in this same area where stimulation can elicit an autonomic "defence reaction" (Carrive et al. 1988).

Conclusion

The projections of the C1 neurons and the nature of their inputs fits with the notion of these cells as prime regulators of autonomic, neuroendocrine and immune reflexes aimed at maintaining homeostasis and preparing the organism for both internal and external threats (for recent review see Guyenet et al. 2013). C1 neurons receive projections relaying information from visceral, somatic and sensory integrative areas and have outputs to both sympathetic and parasympathetic effectors as well as to areas involved in vigilance and neuroendocrine responses. The C1 cells are highly collateralized based on the evidence from the current study as well as previous reports (Mtui et al. 1995; Haselton and Guyenet 1990; Stornetta et al. 1999; Jansen et al. 1995). Stimuli as varied as hypotension, hemorrhage, hypoxia, pain and psychological stress cause fos expression in a large proportion of C1 cells (Chan and Sawchenko 1994; Dayas et al. 2001; Stornetta et al. 2002; Teppema et al. 1997; Li et al. 1998). Our current findings would support that at least the "subsets" of C1 neurons defined by a hypothalamic or spinal projection receive most inputs from similar areas and innervate largely similar regions. Thus, based only on these two sets of projection patterns, we cannot discern any major differences in the wiring of C1 neurons. However, based on the rather small number of neurons we were able to investigate, we cannot dismiss the possibility that some other subsets of C1 neurons are differentially connected and have distinct inputs as well as differing efferent projections.

References

Abbott SB, Stornetta RL, Socolovsky CS, West GH, Guyenet PG (2009) Photostimulation of channelrhodopsin-2 expressing ventrolateral medullary neurons increases sympathetic nerve activity and blood pressure in rats. J Physiol 587(Pt 23):5613–5631

Abbott SB, Kanbar R, Bochorishvili G, Coates MB, Stornetta RL, Guyenet PG (2012) C1 neurons excite locus coeruleus and A5 noradrenergic neurons along with sympathetic outflow in rats. J Physiol 590(Pt 12):2897–2915

Abbott SB, Depuy SD, Nguyen T, Coates MB, Stornetta RL, Guyenet PG (2013) Selective optogenetic activation of rostral ventrolateral medullary catecholaminergic neurons produces cardiorespiratory stimulation in conscious mice. J Neurosci 33:3164–3177

Abbott SB, Holloway BB, Viar KE, Guyenet PG (2014a) Vesicular glutamate transporter 2 is required for the respiratory and parasympathetic activation produced by optogenetic stimulation of catecholaminergic neurons in the rostral ventrolateral medulla of mice in vivo. Eur J Neurosci 39(1):98–106

Abbott SB, Holloway BB, Viar KE, Guyenet PG (2014b) Vesicular glutamate transporter 2 is required for the respiratory and parasympathetic activation produced by optogenetic stimulation

of catecholaminergic neurons in the rostral ventrolateral medulla of mice in vivo. Eur J Neurosci 39(1):98–106

Agassandian K, Shan Z, Raizada M, Sved AF, Card JP (2012) C1 catecholamine neurons form local circuit synaptic connections within the rostroventrolateral medulla of rat. Neuroscience 227:247–259

Aicher SA, Saravay RH, Cravo S, Jeske I, Morrison SF, Reis DJ, Milner TA (1996) Monosynaptic projections from the nucleus tractus solitarii to C1 adrenergic neurons in the rostral ventrolateral medulla: comparison with input from the caudal ventrolateral medulla. J Comp Neurol 373(1):62–75

Aicher SA, Schreihofer AM, Kraus JA, Sharma S, Milner TA, Guyenet PG (2001) Mu-opioid receptors are present in functionally identified sympathoexcitatory neurons in the rat rostral ventrolateral medulla. J Comp Neurol 433:34–47

Burke PG, Abbott SB, Coates MB, Viar KE, Stornetta RL, Guyenet PG (2014) Optogenetic stimulation of adrenergic C1 neurons causes sleep state-dependent cardiorespiratory stimulation and arousal with sighs in rats. Am J Respir Crit Care Med 190(11):1301–1310. doi:10.1164/rccm.201407-1262OC

Callaway EM, Luo L (2015) Monosynaptic circuit tracing with glycoprotein-deleted rabies viruses. J Neurosci 35(24):8979–8985. doi:10.1523/jneurosci.0409-15.2015

Card JP, Sved JC, Craig B, Raizada M, Vazquez J, Sved AF (2006) Efferent projections of rat rostroventrolateral medulla C1 catecholamine neurons: implications for the central control of cardiovascular regulation. J Comp Neurol 499(5):840–859

Card JP, Kobiler O, McCambridge J, Ebdlahad S, Shan Z, Raizada MK, Sved AF, Enquist LW (2011) Microdissection of neural networks by conditional reporter expression from a Brainbow herpesvirus. Proc Natl Acad Sci USA 108(8):3377–3382

Carrive P, Bandler R, Dampney RA (1988) Anatomical evidence that hypertension associated with the defence reaction in the cat is mediated by a direct projection from a restricted portion of the midbrain periaqueductal grey to the subretrofacial nucleus of the medulla. Brain Res 460:339–345

Chan RKW, Sawchenko PE (1994) Spatially and temporally differentiated patterns of c-fos expression in the brainstem catecholaminergic cell groups induced by cardiovascular challenges in the rat. J Comp Neurol 348(3):433–460

Chan RKW, Sawchenko PE (1995) Hemodynamic regulation of tyrosine hydroxylase messenger RNA in medullary catecholamine neurons: a c-fos-guided hybridization histochemical study. Neurosci 66:377–390

Chan RKW, Sawchenko PE (1998) Organization and transmitter specificity of medullary neurons activated by sustained hypertension: implications for understanding baroreceptor reflex circuitry. J Neurosci 18:371–387

Chen D, Bassi JK, Walther T, Thomas WG, Allen AM (2010) Expression of angiotensin type 1A receptors in C1 neurons restores the sympathoexcitation to angiotensin in the rostral ventrolateral medulla of angiotensin type 1A knockout mice. Hypertension 56(1):143–150

Clement CI, Keay KA, Bandler R (1998) Medullary catecholaminergic projections to the ventrolateral periaqueductal gray region activated by halothane anaesthesia. Neuroscience 86(4):1273–1284

Comer AM, Qi J, Christie DL, Gibbons HM, Lipski J (1998) Noradrenaline transporter expression in the pons and medulla oblongata of the rat: localisation to noradrenergic and some C1 adrenergic neurones. Mol Brain Res 62:65–76

Dampney RAL, McAllen RM (1988) Differential control of sympathetic fibres supplying hindlimb skin and muscle by subretrofacial neurones in the cat. J Physiol 395:41–56

Dayas CV, Buller KM, Crane JW, Xu J, Day TA (2001) Stressor categorization: acute physical and psychological stressors elicit distinctive recruitment patterns in the amygdala and in medullary noradrenergic cell groups. Eur J Neurosci 14(7):1143–1152

Dun SL, Ng YK, Brailoiu GC, Ling EA, Dun NJ (2002) Cocaine- and amphetamine-regulated transcript peptide-immunoreactivity in adrenergic C1 neurons projecting to the intermediolateral cell column of the rat. J Chem Neuroanat 23(2):123–132

Erickson JT, Millhorn DE (1994) Hypoxia and electrical stimulation of the carotid sinus nerve induce c-Fos-like immunoreactivity within catecholaminergic and serotinergic neurons of the rat brainstem. J Comp Neurol 348:161–182

Ericsson A, Kovacs KJ, Sawchenko PE (1994) A functional anatomical analysis of central pathways subserving the effects of interleukin-1 on stress-related neuroendocrine neurons. J Neurosci 14(2):897–913

Ericsson A, Arias C, Sawchenko PE (1997) Evidence for an intramedullary prostaglandin-dependent mechanism in the activation of stress-related neuroendocrine circuitry by intravenous interleukin-1. J Neurosci 17(18):7166–7179

Esser MJ, Pronych SP, Allen GV (1998) Trigeminal-reticular connections: possible pathways for nociception-induced cardiovascular reflex responses in the rat. J Comp Neurol 391(4):526–544

Farkas E, Jansen AS, Loewy AD (1998) Periaqueductal gray matter input to cardiac-related sympathetic premotor neurons. Brain Res 792(2):179–192

Farnham MM, Li Q, Goodchild AK, Pilowsky PM (2008) PACAP is expressed in sympathoexcitatory bulbospinal C1 neurons of the brain stem and increases sympathetic nerve activity in vivo. Am J Physiol Regul Integr Comp Physiol 294(4):R1304–R1311

Gluska S, Zahavi EE, Chein M, Gradus T, Bauer A, Finke S, Perlson E (2014) Rabies Virus Hijacks and accelerates the p75NTR retrograde axonal transport machinery. PLoS Pathog 10(8):e1004348. doi:10.1371/journal.ppat.1004348

Guyenet PG, Stornetta RL, Weston MC, McQuiston T, Simmons JR (2004) Detection of amino acid and peptide transmitters in physiologically identified brainstem cardiorespiratory neurons. Auton Neurosci Basic Clin 114(1–2):1–10

Guyenet PG, Stornetta RL, Bochorishvili G, Depuy SD, Burke PG, Abbott SB (2013) C1 neurons: the body's EMTs. Am J Physiol Regul Integr Comp Physiol 305(3):R187–R204. doi:10.1152/ajpregu.00054.2013

Haselton JR, Guyenet PG (1989a) Central respiratory modulation of medullary sympathoexcitatory neurons in rat. Am J Physiol Regul Integr Comp Physiol 256:R739–R750

Haselton JR, Guyenet PG (1989b) Electrophysiological characterization of putative C1 adrenergic neurons in the rat. Neuroscience 30:199–214

Haselton JR, Guyenet PG (1990) Ascending collaterals of medullary barosensitive neurons and C1 cells in rats. Am J Physiol Regul Integr Comp Physiol 258:R1051–R1063

Herbert H, Saper CB (1992) Organization of medullary adrenergic and noradrenergic projections to the periaqueductal gray matter in the rat. J Comp Neurol 315(1):34–52

Holloway BB, Stornetta RL, Bochorishvili G, Erisir A, Viar KE, Guyenet PG (2013) Monosynaptic glutamatergic activation of locus coeruleus and other lower brainstem noradrenergic neurons by the c1 cells in mice. J Neurosci 33(48):18792–18805

Holstein GR, Friedrich VL Jr, Kang T, Kukielka E, Martinelli GP (2011) Direct projections from the caudal vestibular nuclei to the ventrolateral medulla in the rat. Neuroscience 175:104–117. doi:10.1016/j.neuroscience.2010.12.011

Holstein GR, Friedrich VL Jr, Martinelli GP (2014) Projection neurons of the vestibulo-sympathetic reflex pathway. J Comp Neurol 522(9):2053–2074. doi:10.1002/cne.23517

Huangfu D, Verberne AJM, Guyenet PG (1992) Rostral ventrolateral medullary neurons projecting to locus coeruleus have cardiorespiratory inputs. Brain Res 598:67–75

Jansen ASP, Nguyen XV, Karpitskiy V, Mettenleiter TC, Loewy AD (1995) Central command neurons of the sympathetic nervous system: basis of the fight-or flight response. Science 270:644–646

Koji K, Simon M, Tina L, Ann KG, Paul MP (2008) Neuropeptide Y in the rostral ventrolateral medulla blocks somatosympathetic reflexes in anesthetized rats. Auton Neurosci 142(1):64–70

Kwiat GC, Basbaum AI (1990) Organization of tyrosine hydroxylase-immunoreactive and serotonin-immunoreactive brainstem neurons with axon collaterals to the periaqueductal gray and the spinal cord in the rat. Brain Res 528:83–94

Lafon M (2005) Rabies virus receptors. J Neurovirol 11(1):82–87. doi:10.1080/13550280590900427

Li HY, Ericsson A, Sawchenko PE (1996) Distinct mechanisms underlie activation of hypothalamic neurosecretory neurons and their medullary catecholaminergic afferents in categorically different stress paradigms. Proc Natl Acad Sci USA 93:2359–2364

Li T, Gao W, Rao ZR (1998) Noxious somatic stimulation-induced expression of Fos-like immunoreactivity in catecholaminergic neurons with habenular nucleus projection in the medullary visceral zone of rat. Brain Res 783(1):51–56

Li AJ, Wang Q, Dinh TT, Ritter S (2009) Simultaneous silencing of Npy and Dbh expression in hindbrain A1/C1 catecholamine cells suppresses glucoprivic feeding. J Neurosci 29(1):280–287

Li AJ, Wang Q, Davis H, Wang R, Ritter S (2015a) Orexin-A enhances feeding in male rats by activating hindbrain catecholamine neurons. Am J Physiol Regul Integr Comp Physiol 00065:02015. doi:10.1152/ajpregu.00065.2015

Li AJ, Wang Q, Elsarelli MM, Brown RL, Ritter S (2015b) Hindbrain catecholamine neurons activate orexin neurons during systemic glucoprivation in male rats. Endocrinology. doi:10.1210/en.2015-1138

Lipski J, Kanjhan R, Kruszewska B, Smith M (1995) Barosensitive neurons in the rostral ventrolateral medulla of the rat in vivo: morphological properties and relationship to C1 adrenergic neurons. Neuroscience 69(2):601–618

Lonergan T, Goodchild AK, Christie MJ, Pilowsky PM (2003) Mu opioid receptors in rat ventral medulla: effects of endomorphin-1 on phrenic nerve activity. Respir Physiol Neurobiol 138(2–3):165–178

Lovick TA (1992a) Inhibitory modulation of the cardiovascular defence response by the ventrolateral periaqueductal grey matter in rats. Exp Brain Res 89:133–139

Lovick TA (1992b) Midbrain influences on ventrolateral medullo-spinal neurones in the rat. Exp Brain Res 90:147–152

Luppi P-H, Fort P, Kitahama K, Denoroy L, Jouvet M (1989) Adrenergic input from medullary ventrolateral C1 cells to the nucleus raphe pallidus of the cat, as demonstrated by a double immunostaining technique. Neurosci Lett 106(1–2):29–35

Marina N, Abdala AP, Korsak A, Simms AE, Allen AM, Paton JF, Gourine AV (2011) Control of sympathetic vasomotor tone by catecholaminergic C1 neurones of the rostral ventrolateral medulla oblongata. Cardiovasc Res 91(4):703–710

McAllen RM (1985) Mediation of the fastigial pressor reflex and a somatosympathetic reflex by ventral medullary neurones in the cat. J Physiol 368:423–433

McAllen RM, Dampney RA (1990) Vasomotor neurons in the rostral ventrolateral medulla are organized topographically with respect to type of vascular bed but not body region. Neurosci Lett 110:91–96

McAllen RM, May CN, Campos RR (1997) The supply of vasomotor drive to individual classes of sympathetic neuron. Clin Exp Hypertens 19(5–6):607–618

McCulloch PF, Panneton WM (2003) Activation of brainstem catecholaminergic neurons during voluntary diving in rats. Brain Res 984(1–2):42–53

Milner TA, Abate C, Reis DJ, Pickel VM (1989) Ultrastructural localization of phenylethanolamine N-methyltransferase-like immunoreactivity in the rat locus coeruleus. Brain Res 478:1–15

Miyawaki T, Goodchild AK, Pilowsky PM (2002) Activation of mu-opioid receptors in rat ventrolateral medulla selectively blocks baroreceptor reflexes while activation of delta opioid receptors blocks somato-sympathetic reflexes. Neuroscience 109(1):133–144

Mtui EP, Anwar M, Reis DJ, Ruggiero DA (1995) Medullary visceral reflex circuits: local afferents to nucleus tractus solitarii synthesize catecholamines and project to thoracic spinal cord. J Comp Neurol 351:5–26

Mueller PJ, Mischel NA, Scislo TJ (2011) Differential activation of adrenal, renal, and lumbar sympathetic nerves following stimulation of the rostral ventrolateral medulla of the rat. Am J Physiol Regul Integr Comp Physiol 300(5):R1230–R1240. doi:10.1152/ajpregu.00713.2010

Muller-Ribeiro FC, Dampney RA, McMullan S, Fontes MA, Goodchild AK (2014) Disinhibition of the midbrain colliculi unmasks coordinated autonomic, respiratory, and somatomotor responses to auditory and visual stimuli. Am J Physiol Regul Integr Comp Physiol 307(8):R1025–R1035. doi:10.1152/ajpregu.00165.2014

Nicholas AP, Hancock MB (1990) Evidence for projections from the rostral medullary raphe onto medullary catecholamine neurons in the rat. Neurosci Lett 108(1–2):22–28

Panneton WM, Gan Q, Le J, Livergood RS, Clerc P, Juric R (2012) Activation of brainstem neurons by underwater diving in the rat. Front Physiol 3:111

Paton JF, Boscan P, Pickering AE, Nalivaiko E (2005) The yin and yang of cardiac autonomic control: vago-sympathetic interactions revisited. Brain Res Rev 49(3):555–565

Paxinos G, Franklin KBJ (2013) The Mouse Brain in Stereotaxic Coordinates. 4th edn. Academic Press, New York

Pearson RJ, Gatti PJ, Sahibzada N, Massari VJ, Gillis RA (2007) Ultrastructural evidence for selective noradrenergic innervation of CNS vagal projections to the fundus of the rat. Auton Neurosci 136(1–2):31–42

Petrov T, Krukoff TL, Jhamandas JH (1993) Branching projections of catecholaminergic brainstem neurons to the paraventricular hypothalamic nucleus and the central nucleus of the amygdala in the rat. Brain Res 609(1–2):81–92

Pickel VM, Chan J, Park DH, Joh TH, Milner TA (1986) Ultrastructural localization of phenylethanolamine N-methyltransferase in sensory and motor nuclei of the vagus nerve. J Neurosci Res 15(4):439–456

Puskas N, Papp RS, Gallatz K, Palkovits M (2010) Interactions between orexin-immunoreactive fibers and adrenaline or noradrenaline-expressing neurons of the lower brainstem in rats and mice. Peptides 31(8):1589–1597

Pyner S, Coote JH (1994) Evidence that sympathetic preganglionic neurones are arranged in target-specific columns in the thoracic spinal cord of the rat. J Comp Neurol 342:15–22

Ritter S, Llewellyn-Smith I, Dinh TT (1998) Subgroups of hindbrain catecholamine neurons are selectively activated by 2-deoxy-D-glucose induced metabolic challenge. Brain Res 805(1–2):41–54

Ritter S, Bugarith K, Dinh TT (2001) Immunotoxic destruction of distinct catecholamine subgroups produces selective impairment of glucoregulatory responses and neuronal activation. J Comp Neurol 432(2):197–216

Ross CA, Armstrong DM, Ruggiero DA, Pickel VM, Joh TH, Reis DJ (1981) Adrenaline neurons in the rostral ventrolateral medulla innervate thoracic spinal cord: a combined immunocytochemical and retrograde transport demonstration. Neurosci Lett 25:257–262

Ross CA, Ruggiero DA, Joh TH, Park DH, Reis DJ (1984) Rostral ventrolateral medulla: selective projections to the thoracic

autonomic cell column from the region containing C1 adrenaline neurons. J Comp Neurol 228:168–185

Rukhadze I, Kubin L (2007) Differential pontomedullary catecholaminergic projections to hypoglossal motor nucleus and viscerosensory nucleus of the solitary tract. J Chem Neuroanat 33(1):23–33. doi:10.1016/j.jchemneu.2006.10.001

Saper CB, Loewy AD (1980) Efferent connections of the parabrachial nucleus in the rat. Brain Res 197(2):291–317

Sartor DM, Verberne AJ (2003) Phenotypic identification of rat rostroventrolateral medullary presympathetic vasomotor neurons inhibited by exogenous cholecystokinin. J Comp Neurol 465(4):467–479

Sawchenko PE, Bohn MC (1989) Glucocorticoid receptor-immunoreactivity in C1, C2, and C3 adrenergic neurons that project to the hypothalamus or to the spinal cord in the rat. J Comp Neurol 285(1):107–116

Sawchenko PE, Swanson LW (1982) The organization of noradrenergic pathways from the brainstem to the paraventricular and supraoptic nucleus in the rat. Brain ResearchRev 4:275–325

Sawchenko PE, Swanson LW, Grzanna R, Howe PR, Bloom SR, Polak JM (1985) Colocalization of neuropeptide Y immunoreactivity in brainstem catecholaminergic neurons that project to the paraventricular nucleus of the hypothalamus. J Comp Neurol 241(2):138–153

Schreihofer AM, Guyenet PG (1997) Identification of C1 presympathetic neurons in rat rostral ventrolateral medulla by juxtacellular labeling in vivo. J Comp Neurol 387:524–536

Schreihofer AM, Guyenet PG (2002) The baroreflex and beyond: control of sympathetic vasomotor tone by GABAergic neurons in the ventrolateral medulla. Clin Exp Pharm Phys 29(5–6):514–521

Sevigny CP, Bassi J, Teschemacher AG, Kim KS, Williams DA, Anderson CR, Allen AM (2008) C1 neurons in the rat rostral ventrolateral medulla differentially express vesicular monoamine transporter 2 in soma and axonal compartments. Eur J Neurosci 28(8):1536–1544

Stornetta RL (2009) Neurochemistry of bulbospinal presympathetic neurons of the medulla oblongata. J Chem Neuroanat 38(3):222–230

Stornetta RL, Morrison SF, Ruggiero DA, Reis DJ (1989) Neurons of rostral ventrolateral medulla mediate somatic pressor reflex. Am J Physiol 256:R448–R462

Stornetta R, Adam N, Guyenet PG (1990) Neuropeptide Y (NPY) mRNA is co-localized in catecholamine (CA) synthesizing neurons in rat brain. FASEB J 4:A882

Stornetta RL, Akey PJ, Guyenet PG (1999) Location and electrophysiological characterization of rostral medullary adrenergic neurons that contain neuropeptide Y mRNA in rat. J Comp Neurol 415:482–500

Stornetta RL, Schreihofer AM, Pelaez NM, Sevigny CP, Guyenet PG (2001) Preproenkephalin mRNA is expressed by C1 and non-C1 barosensitive bulbospinal neurons in the rostral ventrolateral medulla of the rat. J Comp Neurol 435(1):111–126

Stornetta RL, Sevigny CP, Schreihofer AM, Rosin DL, Guyenet PG (2002) Vesicular glutamate transporter DNPI/GLUT2 is expressed by both C1 adrenergic and nonaminergic presympathetic vasomotor neurons of the rat medulla. J Comp Neurol 444(3):207–220

Stornetta RL, McQuiston TJ, Guyenet PG (2004) GABAergic and glycinergic presympathetic neurons of rat medulla oblongata identified by retrograde transport of pseudorabies virus and in situ hybridization. J Comp Neurol 479(3):257–270

Stornetta RL, Macon CJ, Nguyen TM, Coates MB, Guyenet PG (2013) Cholinergic neurons in the mouse rostral ventrolateral medulla target sensory afferent areas. Brain Struct Funct 218(2):455–475

Teppema LJ, Veening JG, Kranenburg A, Dahan A, Berkenbosch A, Olievier C (1997) Expression of c-fos in the rat brainstem after exposure to hypoxia and to normoxic and hyperoxic hypercapnia. J Comp Neurol 388(2):169–190

Tucker DC, Saper CB, Ruggiero DA, Reis DJ (1987) Organization of central adrenergic pathways: I. Relationships of ventrolateral medullary projections to the hypothalamus and spinal cord. J Comp Neurol 259:591–603

Van Bockstaele EJ, Aston-Jones G, Pieribone VA, Ennis M, Shipley MT (1991) Subregions of the periaqueductal gray topographically innervate the rostral ventral medulla in the rat. J Comp Neurol 309(3):305–327. doi:10.1002/cne.903090303

VanderHorst VG, Ulfhake B (2006) The organization of the brainstem and spinal cord of the mouse: relationships between monoaminergic, cholinergic, and spinal projection systems. J Chem Neuroanat 31(1):2–36

Verberne AJM, Stornetta RL, Guyenet PG (1999) Properties of C1 and other ventrolateral medullary neurones with hypothalamic projections in the rat. J Physiol 517:477–494

Wall NR, Wickersham IR, Cetin A, De La PM, Callaway EM (2010) Monosynaptic circuit tracing in vivo through Cre-dependent targeting and complementation of modified rabies virus. Proc Natl Acad Sci USA 107(50):21848–21853

Weible AP, Schwarcz L, Wickersham IR, Deblander L, Wu H, Callaway EM, Seung HS, Kentros CG (2010) Transgenic targeting of recombinant rabies virus reveals monosynaptic connectivity of specific neurons. J Neurosci 30(49):16509–16513

Westlund KN, Craig AD (1996) Association of spinal lamina I projections with brainstem catecholamine neurons in the monkey. Exp Brain Res 110(2):151–162

Wickersham IR, Finke S, Conzelmann KK, Callaway EM (2007a) Retrograde neuronal tracing with a deletion-mutant rabies virus. Nat Methods 4(1):47–49. doi:10.1038/nmeth999

Wickersham IR, Lyon DC, Barnard RJ, Mori T, Finke S, Conzelmann KK, Young JA, Callaway EM (2007b) Monosynaptic restriction of transsynaptic tracing from single, genetically targeted neurons. Neuron 53(5):639–647

Zanzinger J, Czachurski J, Offner B, Seller H (1994) Somato-sympathetic reflex transmission in the ventrolateral medulla oblongata: spatial organization and receptor types. Brain Res 656:353–358